

# Joule-heating dependence of carbon nanofiber resistance

Hisashi Yabutani<sup>1\*</sup>, Toshishige Yamada<sup>1</sup>, Tsutomu Saito<sup>1,2</sup>, and Cary Y. Yang<sup>1</sup>

<sup>1</sup>Center for Nanostructures, Santa Clara University, 500 El Camino Real, Santa Clara, California, 95053, USA

<sup>2</sup>Hitachi High-Technologies Corporation, Ibaraki, Japan

\*Email: HYabutani@scu.edu

**Abstract** - To assess their potential for interconnect applications, the interplay between electrical and thermal transport in carbon nanofibers (CNFs) under high-current stresses is examined. Electrical properties of CNFs bridging tungsten-deposited gold electrodes are measured. Average voltage is recorded as a function of current in each current stress cycle, and the resulting average resistance is shown to decrease with increasing stressing current. This finding reveals an important effect of Joule heating on the resistance of carbon nanostructures.

**Index Terms** – carbon nanofiber, electrothermal transport, Joule heating

## I. INTRODUCTION

Carbon nanostructures have been extensively investigated as potential next-generation interconnect materials [1-5]. One of the candidates, carbon nanofiber (CNF), is made of a stacked-cone structure surrounded by one or more cylindrical graphene walls [1]. In order to evaluate whether CNFs can indeed replace metal interconnects in sub-30nm integrated circuit technology, understanding the electrical and thermal characteristics of this material is of critical importance.

Recent studies of electrical and thermal characteristics of CNFs have shown that breakdown of CNFs is closely

related to Joule heating [6,7]. We have also shown that how CNF is contacted to the substrate or electrodes determines the CNF breakdown location and maximum current density [8]. For the present study, additional measurements and analyses are carried out on CNFs with W-Au electrodes. Average voltage in each current stress cycle shows a decrease with increasing stressing current (lower resistance as stressing current increases). This decrease in resistance is attributed to the elevated maximum temperature in CNF due to Joule heating, which enhances thermally activated transport in the nanofiber [9].

## II. EXPERIMENT

Two different contacts are shown in Fig. 1(a), drop-cast CNF on Au electrodes and W-deposited Au electrodes. CNFs are grown using plasma-enhanced chemical vapor deposition (PECVD) with Ni catalyst on SiO<sub>2</sub> substrate. The drop-cast CNF-electrode devices revealed resistances ranging from 0.1 to 10 M $\Omega$  [6]. This high resistance is caused by poor contact between the CNF and electrodes. However, if current on the order of 100  $\mu$ A is applied (current stressing), resistance decreases by orders of magnitude, down to 1 to 10 k $\Omega$  range. To form a low-resistance contact, we deposit W on the CNF-electrode contact as shown in Fig. 1(c), using a focused ion beam system with source gas W(CO)<sub>6</sub>. Without current stressing, the resistance is already in the k $\Omega$  range, and is insensitive to subsequent current stressing [7]. This finding demonstrates that the contact is highly stable and its electrical (and thermal) resistance is much lower than that formed by drop-casting CNF on Au. Here we study further the electrothermal transport properties of CNF test devices with W-Au electrodes.

## III. RESULTS AND DISCUSSION

CNF partially supported on SiO<sub>2</sub> between two W-Au electrodes is investigated. Fig. 2(a) shows the pre-stress scanning electron microscopy (SEM) image of this test structure and Fig. 2(b) shows that after a stressing current of 100  $\mu$ A was applied for three minutes. After current stressing, the contacted segment, based on SEM bright-contrast image analysis [5], increases in length as shown in Fig. 2(b), while breakdown occurs at 250  $\mu$ A. Thus, although the 100  $\mu$ A stressing current is insufficient to initiate breakdown of the CNF, it nonetheless increases the fraction of substrate contact segment, resulting in more Joule heat dissipated through the substrate. Heat dissipation at the W-Au electrodes is highly efficient compared to that at the substrate contact, since breakdown always occurs closer to the substrate contact segment [8].

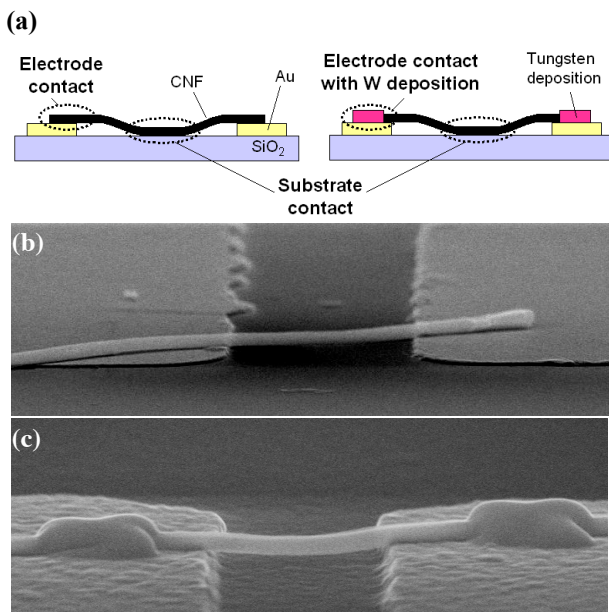


Fig. 1 (a) Schematics of CNF with Au-electrode contacts and CNF with W-Au-electrode contacts. (b) SEM image of CNF with Au electrodes. (c) SEM image of CNF with W-Au electrodes.

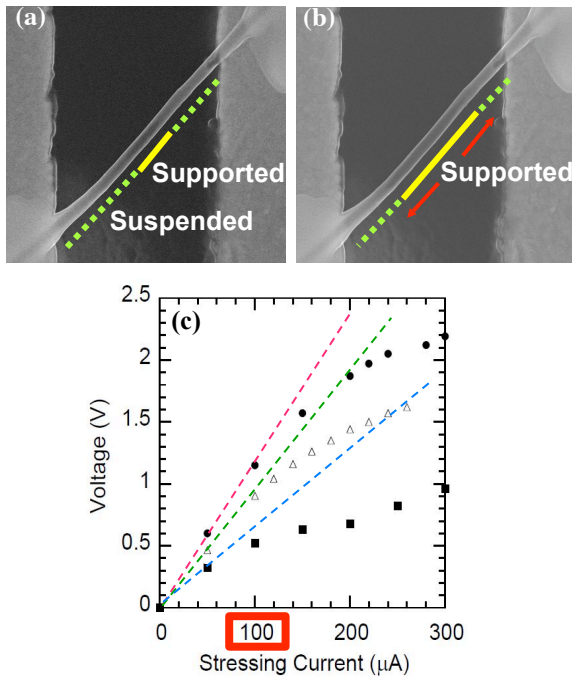


Fig. 2 Changes in CNF due to current stressing. SEM images of the CNF test structure (a) before current stress and (b) after stressing at 100  $\mu\text{A}$ . (c) Observed average voltage as a function of stressing current for three test devices.

For each test device, we apply stressing current progressively, *i.e.*, in the first cycle, a small current is applied for three minutes, and in the second cycle, a slightly larger current is applied for another three minutes, etc. Fig. 2(c) shows the voltage averaged over each stress cycle as a function of stressing current for three test devices. While the stressing current remains constant in each cycle, the voltage reading fluctuates with time and the average voltage is an appropriate measure of the voltage in that cycle. Such voltage measurement is performed at elevated temperature due to Joule heating during the stress cycle. Since the room-temperature resistance after each cycle remains essentially unchanged [7], this decrease in resistance *during current stressing* must reflect the change in bulk CNF properties at elevated temperatures. For each device, below 100  $\mu\text{A}$  stressing current, the voltage varies almost linearly with current, indicating little change in average resistance from one cycle to the next. Above 100  $\mu\text{A}$ , the voltage starts to taper off, and seems to approach saturation at high stressing current. The maximum temperature in the CNF due to Joule heating must increase with stressing current regardless of the elongated supported segment in Fig. 2(b), otherwise breakdown would not occur.

Fig. 3 shows the average resistance computed from Fig. 2(c) as a function of stressing current. Since the amount of Joule heat goes up with increasing stressing current, this plot can be regarded as the qualitative behavior of CNF resistance with increasing temperature. In ref. [7], we performed a complementary experiment, where resistance was measured after stressing current was *turned off* and the CNF was cooled down to room temperature, using much smaller current than in the stress cycle so that Joule heating

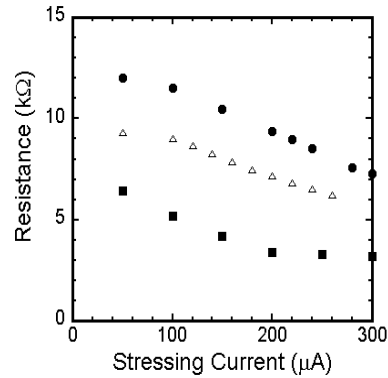


Fig. 3 Average resistance as a function of stressing current obtained from Fig. 2(c) for each of the three test devices.

was negligible. The result showed that resistance as a function of stressing current was almost constant and in the  $\text{k}\Omega$  range [7]. The comparison of these two measurements, combined with our previous findings [5,6], suggests that the resistance change due to Joule heating is mostly entirely due to change in bulk CNF properties at elevated temperatures, *not* contacts, and is reversible once the system returns to room temperature.

The mechanism for CNF bulk resistance decrease with temperature was discussed in the context of transport in disordered media [9]. Our CNF devices have impurities and/or lattice defects, which often serve to trap carriers. Thermal energy releases these carriers from the trap centers, giving rise to lower resistance. Thus transport is controlled by thermal activation of these trapped carriers and their subsequent re-trapping as the temperature is lowered [9]. The same mechanism would account for the decrease in resistance in Fig. 3, as the temperature increases with increasing stressing current due to Joule heating. Resistance reduction with increasing temperature is similar to variable range hopping in disordered materials [10], but the electron wave nature is not expected to be a determining factor in our case, since our measurements are performed at or above room temperature.

#### ACKNOWLEDGMENT

This work was supported by the United States Army Space and Missile Defense Command (SMDC) and carries Distribution Statement A, approved for public release, distribution unlimited.

#### REFERENCES

- [1] Q. Ngo, A. M. Cassell, A. J. Austin, J. Li, S. Krishnan, M. Meyyappan, and C. Y. Yang, *IEEE Electron Device Lett.* **27**, 221 (2006).
- [2] J. Y. Huang, S. Chen, S. H. Jo, Z. Wang, D. X. Han, G. Chen, M. S. Dresselhaus, Z. and F. Ren, *Phys. Rev. Lett.* **94**, 236802 (2005).
- [3] T. D. Yuzvinsky, W. Mickelson, S. Aloni, S. L. Konsek, A. M. Fennimore, G. E. Begtrup, A. Kis, B. C. Regan, and A. Zettl, *Appl. Phys. Lett.* **87**, 083103 (2005).
- [4] E. Pop, D. A. Mann, J. Cao, K. E. Goodson, and H. Dai, *J. Appl. Phys.* **101**, 093710 (2007).
- [5] M. Suzuki, T. Yamada, and C. Y. Yang, *Appl. Phys. Lett.* **90**, 083111 (2007).
- [6] H. Kitsuki, T. Yamada, D. Fabris, J. R. Jameson, P. Wilhite, M. Suzuki, and C. Y. Yang, *Appl. Phys. Lett.* **92**, 173110 (2008).
- [7] T. Saito, T. Yamada, D. Fabris, H. Kitsuki, P. Wilhite, M. Suzuki, and C. Y. Yang, *Appl. Phys. Lett.* **93**, 102108 (2008).

- [8] T. Yamada, T. Saito, D. Fabris, and C. Y. Yang, "Electrothermal Analysis of Breakdown in Carbon Nanofiber Interconnects", to appear in *IEEE Electron Device Lett.* (2009).
- [9] Q. Ngo, T. Yamada, M. Suzuki, Y. Ominami, A. M. Cassell, J. Li, M. Meyyappan, and C.Y. Yang, *IEEE Trans. Nanotechnology* **6**, 688 (2007).
- [10] T. Ando, A. B. Fowler, and F. Stern, *Rev. Mod. Phys.* **54**, 437 (1982).